

## Article

# White Matter Microstructure and Atypical Visual Orienting in 7-Month-Olds at Risk for Autism

Jed T. Elison, Ph.D.

Sarah J. Paterson, Ph.D.

Jason J. Wolff, Ph.D.

J. Steven Reznick, Ph.D.

Noah J. Sasson, Ph.D.

Hongbin Gu, Ph.D.

Kelly N. Botteron, M.D.

Stephen R. Dager, M.D.

Annette M. Estes, Ph.D.

Alan C. Evans, Ph.D.

Guido Gerig, Ph.D.

Heather C. Hazlett, Ph.D.

Robert T. Schultz, Ph.D.

Martin Styner, Ph.D.

Lonnie Zwaigenbaum, M.D.

Joseph Piven, M.D.

for the IBIS Network

**Objective:** The authors sought to determine whether specific patterns of oculomotor functioning and visual orienting characterize 7-month-old infants who later meet criteria for an autism spectrum disorder (ASD) and to identify the neural correlates of these behaviors.

**Method:** Data were collected from 97 infants, of whom 16 were high-familial-risk infants later classified as having an ASD, 40 were high-familial-risk infants who did not later meet ASD criteria (high-risk negative), and 41 were low-risk infants. All infants underwent an eye-tracking task at a mean age of 7 months and a clinical assessment at a mean age of 25 months. Diffusion-weighted imaging data were acquired for 84 of the infants at 7 months. Primary outcome

measures included average saccadic reaction time in a visually guided saccade procedure and radial diffusivity (an index of white matter organization) in fiber tracts that included corticospinal pathways and the splenium and genu of the corpus callosum.

**Results:** Visual orienting latencies were longer in 7-month-old infants who expressed ASD symptoms at 25 months compared with both high-risk negative infants and low-risk infants. Visual orienting latencies were uniquely associated with the microstructural organization of the splenium of the corpus callosum in low-risk infants, but this association was not apparent in infants later classified as having an ASD.

**Conclusions:** Flexibly and efficiently orienting to salient information in the environment is critical for subsequent cognitive and social-cognitive development. Atypical visual orienting may represent an early prodromal feature of an ASD, and abnormal functional specialization of posterior cortical circuits directly informs a novel model of ASD pathogenesis.

(*Am J Psychiatry* 2013; 170:899–908)

**D**evelopmental models of autism spectrum disorders (ASDs) suggest that atypical or biased visual attention patterns in the first year of life could directly contribute to the emergence of the characteristic social-cognitive deficits (1). Indeed, many of the early behavioral markers associated with a later emerging ASD—orienting to name, responding to bids for joint attention, spontaneous gaze to faces, and making eye contact (2–4)—implicate behaviors associated with flexibly allocating attentional resources to salient or biologically relevant information in the environment.

Selective attention refers to the process by which information is channeled, filtered, or enhanced for further processing in higher-order neural systems. It has long been recognized that selective attention shapes the development of adaptive cognitive function (5). Although the neural circuitry of selective attention has been comprehensively delineated in adults (6–10) and selective attention's role in social cognition continues to be elucidated (10, 11), the precise circuitry that underlies selective

visual attention during infancy is unknown. Characterizing the neural correlates of visual attention during infancy may inform our understanding of cortical specialization, as experience with specific categories of information may sculpt neural circuits and enhance processing efficiency (12).

The specialized perception, processing, and evaluation of social information readily observable in typically developing individuals are a source of impairment in individuals with ASDs. Navigating the subtle complexities of social dynamics often requires rapid, flexible, and efficient information processing. But before the actual processing of social information, flexibly orienting gaze and visual attention to the most salient or biologically relevant information in the environment is essential. We reasoned that a deficit in visual orienting during infancy could constrain typical developmental processes leading to specialization with social information, thereby contributing to the emergence of social-communication deficits related to

This article is featured in this month's AJP **Audio** and is the subject of a **CME** course (p. 935)

**TABLE 1. Characteristics of Infants With Low or High Familial Risk of Autism Spectrum Disorders (ASDs), With and Without ASD Symptoms at 24 Months<sup>a</sup>**

Characteristic							Analysis of Variance				Pairwise Group Differences	
							F (df=2, 94)		p		High-Risk-ASD and Low-Risk	High-Risk-ASD and High-Risk-Negative
	Low-Risk (N=41)		High-Risk-Negative (N=40)		High-Risk-ASD (N=16)				p	p		
	N	%	N	%	N	%						
Male <sup>b</sup>	24	58.5	20	50.0	11	68.8						
	Mean	SD	Mean	SD	Mean	SD						
Age at initial visit (months)	7.1	0.8	7.0	0.8	7.2	1.0	0.51	0.604	0.636	0.340		
Mullen Scales of Early Learning <sup>c</sup>												
Early learning composite score	107.8	10.9	105.0	11.7	101.4	12.7	1.81	0.170	0.066	0.300		
Nonverbal developmental quotient	107.4	15.1	106.5	18.5	105.5	11.8	0.08	0.919	0.692	0.833		
Verbal developmental quotient	104.2	15.9	97.0	17.4	93.8	19.5	2.79	0.067	0.044	0.535		
Visual reception standardized score	53.4	7.6	52.8	8.0	52.6	7.3	0.10	0.904	0.725	0.957		
Age at clinical visit (months)	24.8	0.8	25.0	1.1	25.4	1.9	1.57	0.215	0.081	0.200		
Autism Diagnostic Observation Scale <sup>d</sup>												
Social affect subscale score	1.9	1.9	2.0	1.4	11.9	4.1	123.0	<0.001	<0.001	<0.001		
Repetitive behavior subscale score	0.3	0.7	0.6	0.9	2.6	2.0	25.2	<0.001	<0.001	<0.001		
Total score	2.2	2.1	2.6	1.8	14.6	5.5	114.6	<0.001	<0.001	<0.001		

<sup>a</sup> Low-risk=infants with low familial risk; high-risk-negative=infants with high familial risk who did not meet ASD criteria on the Autism Diagnostic Observation Scale (ADOS) at the 24-month clinical visit; high-risk-ASD=infants with high familial risk who met ASD criteria on the ADOS at the 24-month clinical visit.

<sup>b</sup> No significant difference between groups in sex ratio (Fisher's exact test).

<sup>c</sup> In the Mullen Scales of Early Learning, the early learning composite score is a composite of the receptive language, expressive language, fine motor, and visual reception standard scores; the nonverbal developmental quotient is the average age equivalent scores for the fine motor and visual reception subscales divided by chronological age multiplied by 100; the verbal developmental quotient is the average age equivalent scores for the receptive language and expressive language subscales divided by chronological age multiplied by 100.

<sup>d</sup> The ADOS was administered when the child was between 23.6 and 32.7 months of age. The ADOS yields a social affect subscale score and a restricted and repetitive behavior subscale score, and the total ADOS score is the sum of the two subscales. All children in the ASD group met diagnostic criteria for a provisional autism spectrum diagnosis according to the ADOS.

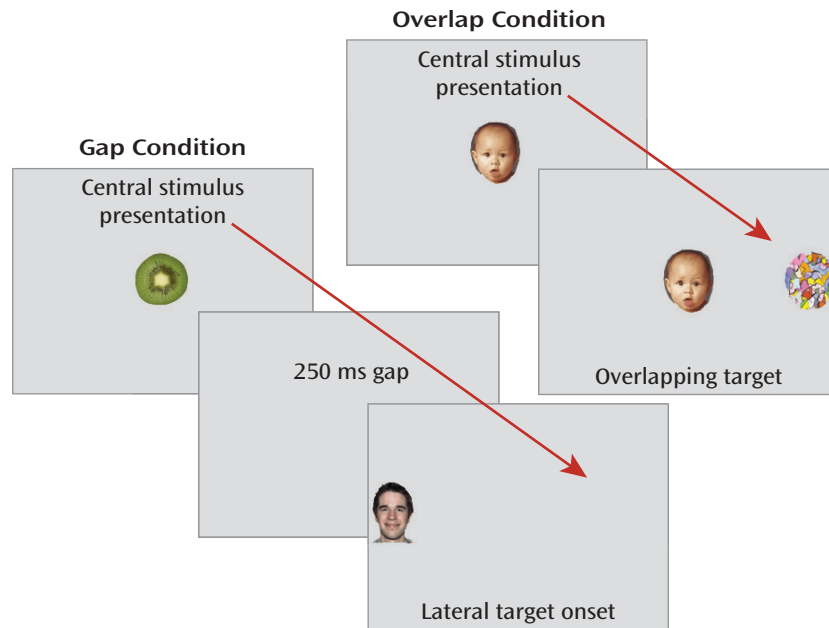
a later diagnosis of ASD. In one study (13), 9- to 10-month-old infants at high familial risk for developing autism (N=16) were reported to have longer visual orienting latencies compared with typically developing low-risk infants. Another study (2) reported that visual orienting latencies measured in a high-risk cohort at 12 months (N=27) correlated with autism symptom severity at 24 months. While these studies informed our hypotheses in this study, critical questions remain as to whether compromised visual orienting behavior is specific to infants who later express an ASD, and if so, how early this behavioral pattern can be detected.

We employed a well-validated visually guided saccade task (the gap/overlap paradigm) to examine saccade latencies in two conditions that represent visual orienting (overlap condition) and oculomotor efficiency (gap condition), respectively. We also used diffusion tensor imaging (DTI) to delineate specific white matter fiber tracts hypothesized to be associated with these behaviors. A recent DTI study reported a unique association between orienting and the splenium of the corpus callosum in adults (9). The splenium is the most posterior sector of the corpus callosum and projects to striate and extrastriate visual areas and to portions of the posterior parietal cortex, including Brodmann's area 7 (14), a cortical target

implicated in sensorimotor programming (15). This tract may function in part as transitional connectivity between extrastriate visual areas and the dorsal frontoparietal and ventral frontoparietal orienting networks identified in adults (10).

Saccadic eye movements that represent oculomotor efficiency, as operationalized in this context, result from temporary inhibition of fixation neurons in the rostral pole of the superior colliculus and disinhibition of the saccade-generating circuit, mediated in part by the reticular formation in the brainstem (16). We therefore hypothesized that individual differences in the organization of white matter fiber bundles projecting from the brainstem to cortical targets (namely, corticospinal tracts) would be associated with individual differences in oculomotor efficiency. Finally, we examined the genu of the corpus callosum as a control tract. The genu projects to frontal association areas associated with voluntary, goal-directed attentional operations (9).

Our goal in this study was to determine whether patterns of oculomotor efficiency and visual orienting in 7-month-olds who are later classified as expressing ASD symptoms are different from those of other infants of similar age. We also examined the neural correlates of task-based behavioral performance and whether the

FIGURE 1. The Modified Gap/Overlap Procedure<sup>a</sup>

<sup>a</sup> During gap trials, a fixation image appeared in the center of a visual display for a variable duration; the central image then disappeared and was followed by a 250-ms temporal gap before a target image appeared in the peripheral visual field (all images subtended a visual angle of 5–7°, visual angle between images subtended 8–10°). During overlap trials, the central image remained present after the appearance of the peripheral target for the duration of the peripheral target presentation (i.e., 2 seconds).

patterns of brain-behavior associations differed between groups.

## Method

### Sample

This study was conducted in the context of an ongoing Autism Center of Excellence Network study prospectively investigating longitudinal brain and behavioral trajectories in high-familial-risk infant siblings of children with ASD and low-risk comparison infants. Infants were considered at high familial risk if they had a biological sibling diagnosed as having an ASD. All infants were enrolled at approximately 6 months of age and underwent a comprehensive behavioral assessment and brain imaging protocol around 6, 12, and 24 months of age (the actual chronological age of children at the time of the visit lagged slightly behind the target visit stages). The data used to investigate the hypotheses in this study include behavioral, imaging, and eye-tracking data from the initial 6-month visit stage and clinical assessment data from the 24-month visit stage. The children were assessed at the University of North Carolina at Chapel Hill and the Children's Hospital of Philadelphia. The research protocol was approved by the institutional review boards at both sites, and parents provided written informed consent after receiving a detailed description of the study. Exclusion criteria for both high-familial-risk and low-familial-risk (hereafter high-risk and low-risk) children included the following: history or physical signs of known genetic conditions or syndromes; significant medical or neurological conditions affecting growth, development, or cognition or sensory impairments such as significant vision or hearing loss; birth weight <2000 g or gestational age <36 weeks, a history of significant perinatal adversity, or in utero exposure to neurotoxins (including alcohol, illicit drugs, and selected prescription medications); a contraindication for MRI;

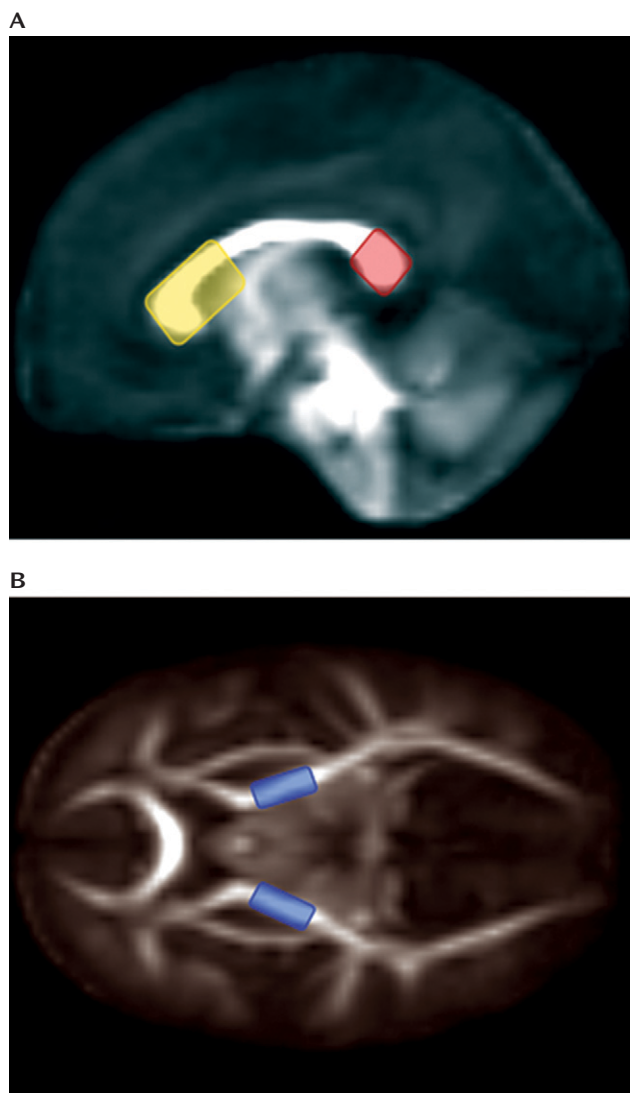
a predominant home language other than English; having been adopted; and a family history of a first-degree relative with an intellectual disability (only for the low-risk group), psychosis, schizophrenia, or bipolar disorder. Low-risk infants were excluded if they had a family history of a first- or second-degree relative with autism or if the low-risk proband (older sibling) showed symptoms of ASD on the Social Communication Questionnaire (17). Clinical diagnosis was corroborated in the proband of high-risk infants with the Autism Diagnostic Interview–Revised (18).

Infants were included in this study if they participated in the eye-tracking protocol during the 6-month visit and had an outcome classification at the 24-month visit. A total of 113 infants were eligible for the study according to these criteria. Fourteen infants did not complete a sufficient number of trials in the eye-tracking task (low-risk group, N=8; high-risk group, N=6) and were excluded from subsequent analyses. These infants did not differ in age or developmental level from those who were included in subsequent analyses. Two infants were enrolled as low-risk but subsequently exceeded the Autism Diagnostic Observation Schedule threshold for an ASD and were excluded from the analyses. The final sample included 97 infants. Table 1 summarizes the sample's characteristics.

### Clinical Assessment

Primary cognitive assessments during the 6-month visit stage included the Mullen Scales of Early Learning (19). ASD classification was made during the 24-month visit with the Autism Diagnostic Observation Scale (ADOS) (20). The ADOS was used to maximize reliable classification of ASD symptoms and was administered and scored by experienced, research-reliable clinicians. A total of 97 infants completed the experimental task and were categorized into three groups based on risk status and ASD classification on the ADOS: low-risk infants (N=41), high-risk infants who did not meet ASD criteria on the ADOS

**FIGURE 2. Regions of Interest for Label Map Seeding in a Study of White Matter Microstructure and Visual Orienting in Infants at Risk for Autism<sup>a</sup>**



<sup>a</sup> Panel A shows regions of interest for the genu (yellow) and splenium (red) of the corpus callosum as applied to the centermost sagittal slice of the study atlas. Panel B shows axial regions of interest for left and right corticospinal white matter passing through the posterior limb of the internal capsule.

(high-risk-negative group, N=40), and high-risk infants who met ADOS criteria for an ASD (high-risk-ASD group, N=16). Seven infants in the low-risk group, four in the high-risk-negative group, and two in the high-risk-ASD group contributed valid eye-tracking data but did not contribute valid imaging data, leaving 84 infants with valid imaging data and eye-tracking data.

### Eye-Tracking Procedure

We measured overt stimulus-driven orienting during visually guided saccade trials in which the timing of the fixation offset and target-stimulus onset was manipulated to examine oculomotor efficiency and visual orienting (Figure 1). Eye movements were recorded with corneal-reflection binocular eye-tracking equipment (Tobii models 1750 and x120, recordings sampled at 50 and 60 Hz, respectively; Tobii Technology, Danderyd, Sweden).

The primary dependent measure was latency to initiate a saccade away from the center image (or center of the display in the gap condition) in the correct direction of the target. Average saccadic latency in the gap condition represents raw oculomotor efficiency. The offset of the fixation stimulus primes the oculomotor system and results in the temporary inhibition of fixation neurons in the rostral pole of the superior colliculus and disinhibition of the saccade-generating circuit, mediated in part by the reticular formation in the brainstem (16). Individual differences in average gap latency stem in part from the relative computational efficiency of these circuits; hence, we refer to “oculomotor efficiency” when describing saccadic latencies in the gap condition. Average saccadic latency in the overlap condition encapsulates a combination of oculomotor responding and attentional orienting (disengaging and shifting attention). Overlap latencies are consistently longer than gap latencies, likely resulting from 1) additional processing demands supported by the lateral intraparietal area (16, 21, 22) and 2) the absence of the fixation offset priming effects. We refer to saccadic latencies in the overlap condition as “visual orienting,” as this concept subsumes both attentional and oculomotor components.

This study was primarily concerned with domain-general response patterns, as there is evidence to suggest that 6-month-old infants who later develop ASD exhibit patterns of “gaze to faces” and “gaze to objects” similar to those of 6-month-olds who do not develop ASD (4). Therefore, we included a variety of complex stimuli (parametrically varied among central and peripheral locations) that included 10 distinct faces and 10 distinct objects. Trials were counterbalanced with no direction (i.e., left or right), condition (i.e., gap or overlap), or central or peripheral stimulus type, respectively (i.e., faces or objects) occurring on more than three consecutive trials. More information about the procedure is available in the data supplement that accompanies the online edition of this article.

### Imaging Protocol

Diffusion-weighted images were acquired during natural sleep on a Siemens 3-T TIM Trio scanner (Siemens, Munich) equipped with a 12-channel head coil using the following parameters: field of view=190 mm, 75 transversal slices, slice thickness=2 mm isotropic,  $2 \times 2 \times 2$  mm<sup>3</sup> voxel resolution, TR=12800 ms, TE=102 ms, b values of 0 to 1000 s/mm<sup>2</sup>, 25 gradient directions, and 4- to 5-minute scan time. Image data were screened for motion and common artifacts using the DTIprep program ([www.nitrc.org/projects/dtiprep](http://www.nitrc.org/projects/dtiprep)), and expert raters manually removed scans with residual artifacts.

### Computational Anatomy Mapping

Image registration proceeded in two steps (23). First, linear affine registration of baseline images was applied to the structurally weighted T<sub>2</sub> atlas using B-spline registration and normalized mutual information (24). Second, a large deformation diffeomorphic metric mapping transformation was applied for unbiased, deformable atlas building (25). The procedure related each individual data set to the study-specific atlas template via a nonlinear, invertible transformation, providing a precise match between the reference atlas and individual image data. Tensor maps were calculated from each data set using weighted least squares estimation (26) and were transformed into the atlas space with tensor reorientation by a finite strain approach (27). Diffusion tensor images were transformed and averaged using the Riemannian and log-Euclidean frameworks (28), resulting in the final three-dimensional average tensor atlas.

### Segmentation and Parameterization of Fiber Tracts

Deterministic tractography was performed by manually drawing seed label maps for the splenium and genu of the

TABLE 2. Summary of Performance in the Gap/Overlap Paradigm<sup>a</sup>

Measure	Low-Risk (N=41)		High-Risk-Negative (N=40)		High-Risk-ASD (N=16)		Analysis of Variance		Pairwise Group Differences <sup>b</sup>			
	Mean	SD	Mean	SD	Mean	SD	F (df=2, 94)	p	High-Risk-ASD and Low-Risk		High-Risk-ASD and High-Risk-Negative	
									p	d	p	d
Valid overlap trials	11.9	6.0	13.5	5.9	11.2	4.1	1.30	0.28				
Valid gap trials	12.9	5.7	14.1	5.1	12.1	4.9	0.93	0.40				
Overlap saccade rate <sup>c</sup>	331	110	322	139	383	161	1.28	0.28				
Gap saccade rate <sup>c</sup>	371	127	343	150	362	185	0.36	0.70				
Overlap latency <sup>d</sup>	412.6	59.0	404.9	72.5	454.6	62.2	3.42	0.04	0.03	0.71	0.01	0.73
Gap latency <sup>d</sup>	271.4	36.9	287.5	42.1	298.4	42.9	3.14	0.05	0.03	0.71	0.36	0.26
Overlap CoV <sup>e</sup>	0.28	0.10	0.29	0.08	0.30	0.09	0.60	0.55				
Gap CoV <sup>e</sup>	0.17	0.08	0.20	0.10	0.19	0.09	0.74	0.48				
Gap effect <sup>f</sup>	141	55.3	117	64.1	156	56.3	3.00	0.06	0.39	0.27	0.03	0.64
Late or no saccade <sup>g</sup>	1.20	1.57	1.83	2.12	2.13	2.00	1.85	0.16				

<sup>a</sup> Low-risk=infants with low familial risk; high-risk-negative=infants with high familial risk who did not meet ASD criteria on the Autism Diagnostic Observation Scale (ADOS) at 24 months; high-risk-ASD=infants with high familial risk who met ASD criteria on the ADOS at 24 months.

<sup>b</sup> Effect size based on Cohen's d, using pooled variance as the denominator.

<sup>c</sup> Average saccade rate/velocity (in degrees/second) for overlap trials and gap trials. A minimum velocity threshold was set at 80°/second.

<sup>d</sup> Average latency (in ms) to initiate saccade toward the lateral target in the overlap condition and the gap condition.

<sup>e</sup> Coefficient of variation (CoV) for saccade latencies in the overlap condition and the gap condition. The CoV is a standardized index of dispersion or variability and is derived by estimating the ratio of the standard deviation to the mean for each individual.

<sup>f</sup> The gap effect value represents the difference (in ms) between average overlap latency and average gap latency. While it is a common metric extracted from this task, the gap effect value violates the assumption of pure insertion, as there is likely more than one cognitive/neural component active in one condition and not the other.

<sup>g</sup> "Late or no saccade" represents the number of trials that were excluded because the infant failed to initiate a saccade toward the lateral target between 100 and 1000 ms after the onset of the lateral target. This value also includes saccades that were more than two standard deviations from the mean, which always fell at the upward end of the distribution.

corpus callosum and the left and right corticospinal tracts (broadly defined as corticospinal pathways passing through the posterior limb of the internal capsule) based on methods described previously (29) using the 3DSlicer program ([www.slicer.org](http://www.slicer.org)) (Figure 2). Seed spacing was set at 1 mm and proceeded bidirectionally with a linear measure stopping value of 0.1. Extracted fiber tracts were processed for spurious or incomplete streamlines using a software program developed in-house (FiberViewer; [www.ia.unc.edu/dev/](http://www.ia.unc.edu/dev/)). Fiber tracts were converted to binary regions of interest and mapped to individual data sets to generate scalar diffusion measures (i.e., radial diffusivity, axial diffusivity, and fractional anisotropy) along each fiber bundle, from which mean values were derived. We initially chose to focus on radial diffusivity because there have been reports linking this metric to myelination (30), and the relative myelin content is thought to support rapid and efficient signal transmission (31) and therefore efficient information processing. However, there is evidence to suggest that the density and diameter of axons in a given fiber tract, in addition to myelin content, affect the diffusion of water molecules perpendicular to the primary eigenvector of a fiber tract (32). Radial diffusivity was calculated in the conventional manner as the mean of the second and third eigenvalues ( $(\lambda_2 + \lambda_3)/2$ ). To supplement analyses of radial diffusivity reported below, we also examined axial diffusivity and the composite index, fractional anisotropy. The results from these additional analyses are reported in the online data supplement.

## Results

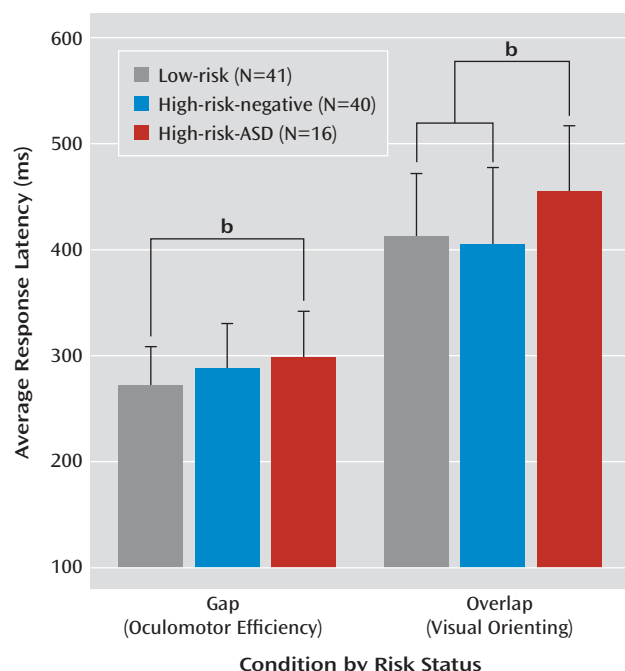
The sex ratio did not differ significantly across the three groups of children, and the groups did not differ statistically in age at the initial 6-month visit, age at the 24-month clinical visit, nonverbal developmental quotient as

measured by the Mullen Scales of Early Learning at the 6-month visit, or standardized score on the visual reception subscale of the Mullen Scales of Early Learning at the 6-month visit.

A multivariate analysis of variance that included gap latency and overlap latency as dependent variables and risk status (low-risk, high-risk-negative, and high-risk-ASD) as the independent variable was statistically significant (Wilks's lambda=0.879;  $F=3.097$ ,  $df=4, 188$ ,  $p=0.017$ ;  $\eta_p^2=0.062$ ). The statistical model also revealed a significant main effect of risk status on both gap latencies ( $F=3.14$ ,  $df=2, 94$ ,  $p=0.048$ ;  $\eta_p^2=0.063$ ) and overlap latencies ( $F=3.42$ ,  $df=2, 94$ ,  $p=0.037$ ;  $\eta_p^2=0.068$ ). Planned post hoc comparisons revealed that the high-risk-ASD group showed significantly longer gap latencies than the low-risk group ( $d=0.71$ ,  $p=0.025$ ) and that the high-risk-negative group did not differ significantly from the low-risk or high-risk-ASD groups. Considering the overlap condition, the high-risk-ASD group showed significantly longer latencies than both the high-risk-negative group ( $d=0.73$ ,  $p=0.012$ ) and the low-risk group ( $d=0.71$ ,  $p=0.032$ ). The low-risk and high-risk-negative groups showed statistically equivalent overlap latencies. Table 2 and Figure 3 summarize performance on the gap/overlap task.

Next, we tested the specificity of the association between average saccadic latencies in the gap condition and white matter fiber tracts that transmit information to and from the brainstem (i.e., the corticospinal tract) and the association between average saccadic latencies in the overlap condition and the splenium of the corpus callosum. To accomplish

**FIGURE 3. Group Differences in Oculomotor and Visual Orienting Behavior in 7-Month-Olds<sup>a</sup>**



<sup>a</sup> Low-risk=infants with low familial risk; high-risk-negative=infants with high familial risk who did not meet autism spectrum disorder (ASD) criteria on the Autism Diagnostic Observation Scale (ADOS) at the 24-month clinical visit; high-risk-ASD=infants with high familial risk who met ASD criteria on the ADOS at the 24-month clinical visit. In the gap condition, latencies for the three groups appear to represent a trend toward a familial marker model. In the overlap condition, latencies for the three groups conformed to a disorder-specific model of impairment (i.e., high-risk-ASD > high-risk-negative = low-risk). Error bars indicate standard deviations.

<sup>b</sup> Least significant difference pairwise group differences,  $p < 0.05$ .

this, we also examined the association between the saccadic latencies and the genu of the corpus callosum to confirm the specificity of any observed association with the splenium or the corticospinal tracts. We report results using radial diffusivity and provide additional data on fractional anisotropy and axial diffusivity when relevant. The analytic strategy (see also reference 9) began with an examination of the zero-order correlation matrix (see graphical representation in Figure 4) and followed with hierarchical multiple regression analyses. The scalar index of the fiber tract of interest was entered into the model as the dependent variable, age and the behavioral response unrelated to the fiber tract were entered as step 1 predictor variables, and the behavioral response hypothetically related to the fiber tract was entered as a step 2 predictor variable.

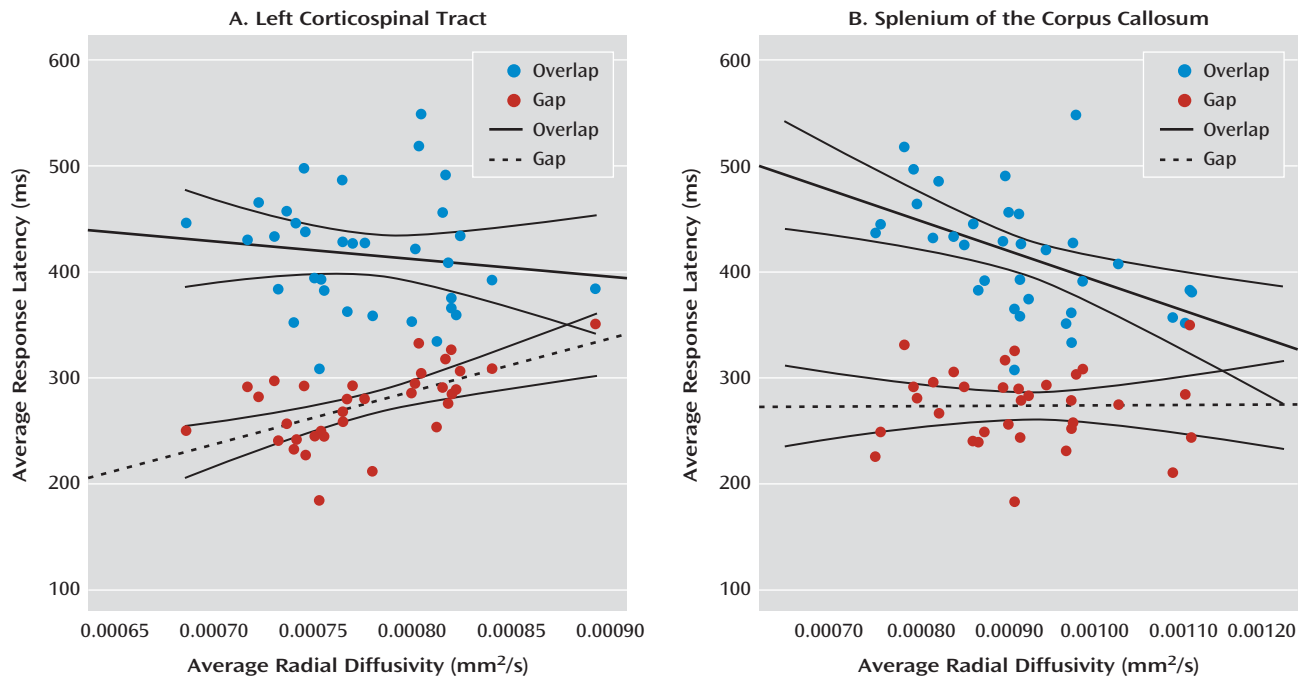
These analyses verified that performance in the two conditions of the gap/overlap procedure was related to dissociable white matter fiber tracts in low-risk infants (N=34; mean age, 31.0 months [SD=3.5]). Average latency in the gap condition accounted for a significant portion of variance in radial diffusivity in the left corticospinal tract ( $\Delta R^2=0.486$ ,  $p < 0.001$ ) beyond the contribution of age and

overlap latency. Average latency in the overlap condition accounted for a significant portion of variance in radial diffusivity in the splenium beyond the contribution of age and gap latency ( $\Delta R^2=0.297$ ,  $p=0.001$ ). Gap latencies did not account for a significant portion of variance in the splenium, and overlap latencies did not account for a significant portion of variance in the left corticospinal tract. There was no association between latencies in the gap/overlap procedure and our control tract, the genu of the corpus callosum (see Figure S2 in the online data supplement). All of these patterns remained when we examined fractional anisotropy and axial diffusivity (see the data supplement), except that gap latencies did not account for a significant portion of the variance in fractional anisotropy in the left corticospinal tract ( $\Delta R^2=0.097$ ,  $p=0.076$ ) beyond the effect of age and overlap latency. However, the trend toward statistical significance is consistent with the results from radial and axial diffusivity.

Considering the pattern of results in the overlap condition (high-risk-ASD > high-risk-negative = low-risk), alongside the finding that overlap latencies (visual orienting) are associated with the splenium in low-risk infants, directly informed the final question: Do the functional properties of the splenium explain the increased overlap latencies observed in infants who later express ASD symptoms? We employed a general linear model that included overlap latencies as the dependent variable and group, radial diffusivity in the splenium, and a group-by-splenium interaction term as independent variables. Group status moderated the association between white matter microstructure in the splenium and overlap latencies. The overall model was significant ( $F=2.82$ ,  $df=5$ ,  $78$ ,  $p=0.021$ ). Additionally, the results revealed a main effect of group ( $F=4.16$ ,  $df=2$ ,  $78$ ,  $p=0.019$ ;  $\eta_p^2=0.096$ ) as well as a significant group-by-splenium interaction ( $F=4.53$ ,  $df=2$ ,  $78$ ,  $p=0.014$ ;  $\eta_p^2=0.104$ ). Average radial diffusivity in the splenium did not differ between groups. The significant interaction indicates that the association between brain and behavior varies by group. The simple slope for the low-risk group significantly differed from the simple slope for the high-risk-ASD group ( $t=-2.95$ ,  $p=0.004$ ). The simple slope for the high-risk-negative group did not differ significantly from the low-risk group or the high-risk-ASD group (Figure 5). This pattern of results, and specifically the significant difference in simple slopes between the low-risk group and the high-risk-ASD group, is corroborated by analyses conducted with axial diffusivity (see the online data supplement). For additional results regarding the moderating effect of group status on the association between gap latencies and the left corticospinal tract, see Figures S3 and S5 in the data supplement.

## Discussion

One underlying theme of this study was to elucidate mutually informative findings regarding both typical and atypical development processes. This is among the first

FIGURE 4. Brain-Behavior Double Dissociation in 7-Month-Olds at Low Risk for Autism (N=34)<sup>a</sup>

<sup>a</sup> In panel A, regression lines within the scatterplot represent the zero-order correlation between radial diffusivity in the left corticospinal tract and overlap latencies (blue circles;  $r = -0.128$ ,  $p = 0.472$ ) and gap latencies (red circles;  $r = 0.592$ ,  $p < 0.001$ ), respectively. See Figure S1 in the online data supplement for results on the right corticospinal tract. In panel B, regression lines within the scatterplot represent the zero-order correlation between radial diffusivity in the splenium and overlap latencies (blue circles;  $r = -0.499$ ,  $p = 0.003$ ) and gap latencies (red circles;  $r = 0.006$ ,  $p = 0.975$ ), respectively.

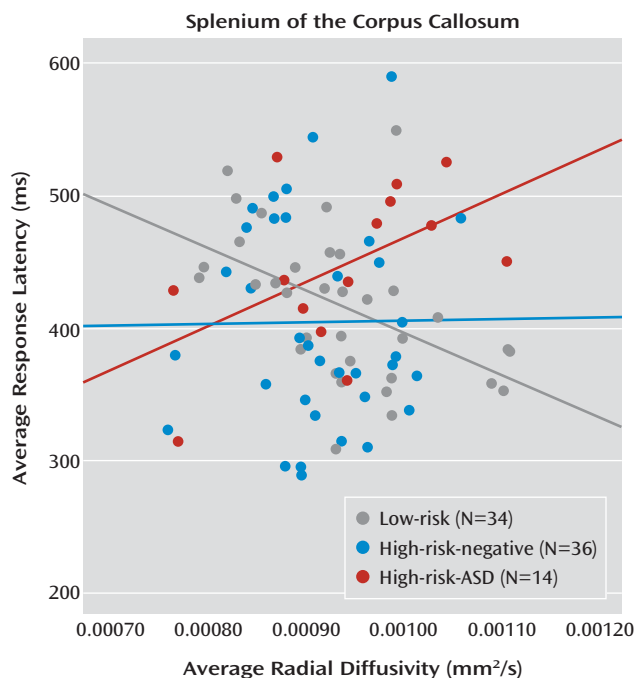
studies to characterize an association between specific white matter fiber tracts and specific behavioral patterns in typically developing infants, an approach that lends itself to inferences regarding functional circuits during infancy. Our results suggest that among typically developing infants, individual differences in visual orienting are associated with individual differences in white matter microstructure of the splenium of the corpus callosum. Visual orienting latencies were not related to the microstructure of the corticospinal tracts, nor were they associated with the anterior segment of the corpus callosum, the genu. Supporting our claims of specificity, oculomotor efficiency, as represented by saccadic latencies in the gap condition, was significantly associated with white matter microstructure in the corticospinal tracts, but not associated with white matter in the splenium or the genu of the corpus callosum. This pattern is consistent with studies examining DTI-related associations with attentional operations in adults (9), as well as behavioral evidence from a rare infant hemispherectomy patient (33).

The internal capsule and the corticospinal tracts myelinate earlier than cortical and commissural tracts (34), and the splenium undergoes more postnatal axonal elimination than any other sector of the corpus callosum (35), a process that likely extends into the sixth or seventh postnatal month in human infants. Therefore, different biophysical mechanisms could affect the diffusion of water

molecules in the corticospinal tracts and the splenium at different ages—namely, density in the splenium and myelination in the corticospinal tract—and thus lead to different directions of association with target behaviors. Considering the density of axons as the primary constraint on water diffusion in the splenium facilitates interpretation of the negative association with visual orienting latencies. A greater density of axons (a proportion of which will subsequently be selectively eliminated) should yield less radial diffusion and could reflect a less mature and less efficient information processing system, resulting in slower reaction times. However, this putative interpretation should be qualified by a growing literature that promotes extreme caution when making inferences about the underlying tissue structure that constrains water diffusion along and across fiber bundles (36). Future research using targeted imaging pulse sequences (34) has the potential to elucidate specific neuroanatomical mechanisms that underlie information processing during infancy.

Previous research has shown that visual orienting latencies are related to encoding speed in 4-month-olds (37), which subsequently predicts cognitive outcomes in preschool-age children (38). Our results here reveal a disorder-specific deficit in visual orienting, such that infants who later express ASD symptoms show significantly longer latencies than both high-risk-negative and

**FIGURE 5. Functional Coupling Between Visual Orienting and the Splenium<sup>a</sup>**



<sup>a</sup> Low-risk=infants with low familial risk; high-risk-negative=infants with high familial risk who did not meet autism spectrum disorder (ASD) criteria on the Autism Diagnostic Observation Scale (ADOS) at the 24-month clinical visit; high-risk-ASD=infants with high familial risk who met ASD criteria on the ADOS at the 24-month clinical visit. Group membership significantly moderates the association between individual differences in radial diffusivity in the splenium and average saccadic latency in the overlap condition.

low-risk infants. By extension, these data suggest that flexible and efficient visual orienting may also be important for typical patterns of social-cognitive development. Furthermore, these results indicate that the functional coupling between visual orienting and white matter microstructure of the splenium observed in low-risk infants differs significantly from high-risk infants who later express ASD symptoms. More research is needed to explicate the precise neural mechanisms that underlie increased visual orienting latencies observed in infants who later express ASD, but our results suggest that the functional efficiency of the splenium and the posterior heteromodal association areas may be critical.

With regard to oculomotor efficiency, or performance in the gap condition, the difference between low-risk and high-risk-ASD infants was quite large and statistically significant, which suggests a marked deficit in the saccade-generating circuit (16, 22). However, these behavioral differences were not explained by variability in the white matter microstructure in the corticospinal tracts (see Figure S3 in the online data supplement), suggesting that a more focused methodological approach is necessary to characterize the neural mechanism that mediates atypical oculomotor functioning in ASD. It is interesting that the

high-risk-negative and high-risk-ASD groups showed statistically equivalent gap latencies. When coupled with the trend toward a significant difference between high-risk-negative and low-risk infants ( $d=0.41$ ,  $p=0.074$ ), this pattern of results suggests that abnormal oculomotor functioning may be a familial marker of ASD (39).

Identifying infants at highest risk for ASD before the consolidation of syndromic features offers the possibility of implementing behavioral and other interventions during infancy that could reduce or prevent the manifestation of the full syndrome (40). The present behavioral findings not only complement and extend recent data suggesting early functional and structural brain abnormalities in infants who go on to develop ASD (41, 42), they also have the potential to enhance early identification of individuals with ASD and to inform targeted interventions developed for the ASD prodrome. Notably, one recent study successfully altered visual orienting performance in 11-month-olds using several gaze-contingent attention training procedures administered during five lab visits over 15 days (43). One of the pre- and posttest procedures that tracked changes due to training was nearly identical to the gap/overlap procedure used in the present study. Additional research is needed to determine the long-term effects of modifying visual orienting patterns in infancy, specifically in relation to how training attention at specific time intervals during infancy might alter social-cognitive development.

Several limitations of this study should be mentioned. First, we used the ADOS at the 24-month visit to classify infants as either presenting ASD symptoms or not. It is currently unknown whether toddlers who show ASD symptoms at 24 months will continue to show symptoms at 3 or 4 years of age. Additionally, increasing the number of high-risk infants would afford the opportunity to examine heterogeneity within the high-risk-ASD group, as well as potential compensatory mechanisms and heterogeneity in the high-risk-negative group. Lastly, radial and axial diffusivity and fractional anisotropy represent indices of white matter microstructure but do not represent the organization of any one specific neurobiological component (e.g., myelin content). Multimodal imaging will be imperative to definitively characterize the neural mechanisms that underlie the emergence of ASD symptoms.

Presented in part at the International Meeting for Autism Research, Toronto, May 17–19, 2012. Received Sept. 2, 2012; revisions received Nov. 9 and Dec. 11, 2012; accepted Dec. 17, 2012 (doi: 10.1176/appi.ajp.2012.12091150). From the Carolina Institute for Developmental Disabilities and the Departments of Psychiatry, Psychology, and Computer Science, University of North Carolina at Chapel Hill; Division of Humanities and Social Sciences, California Institute of Technology, Pasadena; Center for Autism Research, Children’s Hospital of Philadelphia and University of Pennsylvania, Philadelphia; School of Behavioral and Brain Sciences, University of Texas at Dallas; Department of Psychiatry, Washington University, St. Louis; Departments of Radiology and Speech and Hearing Sciences, University of Washington, Seattle; Montreal Neurological Institute,



McGill University, Montreal; Scientific Computing and Imaging Institute, University of Utah, Salt Lake City; Department of Pediatrics, University of Alberta, Edmonton. Address correspondence to Dr. Elison (jelison@caltech.edu) or Dr. Piven (jpiven@med.unc.edu).

Dr. Evans is cofounder of and holds equity in Biospective, Inc.; he has also received consulting fees from Johnson & Johnson and Pfizer. Dr. Hazlett has received travel support from Autism Speaks. All other authors report no financial relationships with commercial interests.

Supported by grants awarded to Dr. Piven from NIH/National Institute of Child Health and Development (NICHD) (Autism Center of Excellence, R01 HD055741 and HD055741-S1; Intellectual and Developmental Disabilities Research Center, P30 HD03110 and T32 HD40127), Autism Speaks, and the Simons Foundation. Dr. Elison was supported by a National Research Service Award (5-T32-HD007376) from NICHD, and aspects of this work contributed to his doctoral dissertation. Further support was provided by the National Alliance for Medical Image Computing, funded by NIH through grant U54 EB005149.

The Infant Brain Imaging Study (IBIS) Network is an NIH-funded Autism Center of Excellence project and consists of a consortium of seven universities in the United States and Canada. Clinical sites: University of North Carolina: J. Piven (IBIS Network principal investigator), H.C. Hazlett, and J.C. Chappell; University of Washington: S. Dager, A. Estes, and D. Shaw; Washington University: K. Botteron, R. McKinstry, J. Constantino, and J. Pruett; Children's Hospital of Philadelphia: R. Schultz and S. Paterson; University of Alberta: L. Zwaigenbaum; Data Coordinating Center: Montreal Neurological Institute: A.C. Evans, D.L. Collins, G.B. Pike, P. Kostopolous, and S. Das; Image Processing Core: University of Utah: G. Gerig; University of North Carolina: M. Styner; Statistical Analysis Core: University of North Carolina: H. Gu; Genetics Analysis Core: University of North Carolina: P. Sullivan and F. Wright.

The authors thank the IBIS children and families for their ongoing participation in this longitudinal study. They also thank Ryan Scotton, Rachel G. Smith, Samir Das, and Penelope Kostopoulos for their efforts and Matt Mosconi, Keize Izuma, and Ralph Adolphs for their comments on the manuscript.

## References

- Klin A, Lin DJ, Gorrindo P, Ramsay G, Jones W: Two-year-olds with autism orient to non-social contingencies rather than biological motion. *Nature* 2009; 459:257–261
- Zwaigenbaum L, Bryson S, Rogers T, Roberts W, Brian J, Szatmari P: Behavioral manifestations of autism in the first year of life. *Int J Dev Neurosci* 2005; 23:143–152
- Landa RJ, Holman KC, Garrett-Mayer E: Social and communication development in toddlers with early and later diagnosis of autism spectrum disorders. *Arch Gen Psychiatry* 2007; 64: 853–864
- Ozonoff S, Iosif AM, Baguio F, Cook IC, Hill MM, Hutman T, Rogers SJ, Rozga A, Sangha S, Sigman M, Steinfeld MB, Young GS: A prospective study of the emergence of early behavioral signs of autism. *J Am Acad Child Adolesc Psychiatry* 2010; 49:256–266.e2
- Kagan J: Attention and psychological change in the young child. *Science* 1970; 170:826–832
- Posner MI, Petersen SE: The attention system of the human brain. *Annu Rev Neurosci* 1990; 13:25–42
- Desimone R, Duncan J: Neural mechanisms of selective visual attention. *Annu Rev Neurosci* 1995; 18:193–222
- Fan J, McCandless BD, Fossella J, Flombaum JI, Posner MI: The activation of attentional networks. *Neuroimage* 2005; 26:471–479
- Niogi S, Mukherjee P, Ghajar J, McCandless BD: Individual differences in distinct components of attention are linked to anatomical variations in distinct white matter tracts. *Front Neuroanat* 2010; 4:2
- Corbetta M, Patel G, Shulman GL: The reorienting system of the human brain: from environment to theory of mind. *Neuron* 2008; 58:306–324
- Vuilleumier P: How brains beware: neural mechanisms of emotional attention. *Trends Cogn Sci* 2005; 9:585–594
- Leppänen JM, Nelson CA: Tuning the developing brain to social signals of emotions. *Nat Rev Neurosci* 2009; 10:37–47
- Elsabbagh M, Volein A, Holmboe K, Tucker L, Csibra G, Baron-Cohen S, Bolton P, Charman T, Baird G, Johnson MH: Visual orienting in the early broader autism phenotype: disengagement and facilitation. *J Child Psychol Psychiatry* 2009; 50:637–642
- Putnam MC, Steven MS, Doron KW, Riggall AC, Gazzaniga MS: Cortical projection topography of the human splenium: hemispheric asymmetry and individual differences. *J Cogn Neurosci* 2010; 22:1662–1669
- Duhamel J-R, Colby CL, Goldberg ME: The updating of the representation of visual space in parietal cortex by intended eye movements. *Science* 1992; 255:90–92
- Dorris MC, Munoz DP: A neural correlate for the gap effect on saccadic reaction times in monkey. *J Neurophysiol* 1995; 73: 2558–2562
- Berument SK, Rutter M, Lord C, Pickles A, Bailey A: Autism screening questionnaire: diagnostic validity. *Br J Psychiatry* 1999; 175:444–451
- Lord C, Rutter M, Le Couteur A: Autism Diagnostic Interview–Revised: a revised version of a diagnostic interview for caregivers of individuals with possible pervasive developmental disorders. *J Autism Dev Disord* 1994; 24:659–685
- Mullen EM: Mullen Scales of Early Learning, AGS Edition. Circle Pines, Minn, American Guidance Services Publishing, 1995
- Lord C, Risi S, Lambrecht L, Cook EH Jr, Leventhal BL, DiLavore PC, Pickles A, Rutter M: The Autism Diagnostic Observation Schedule–Generic: a standard measure of social and communication deficits associated with the spectrum of autism. *J Autism Dev Disord* 2000; 30:205–223
- Posner MI, Walker JA, Friedrich FJ, Rafal RD: Effects of parietal injury on covert orienting of attention. *J Neurosci* 1984; 4:1863–1874
- Corbetta M: Frontoparietal cortical networks for directing attention and the eye to visual locations: identical, independent, or overlapping neural systems? *Proc Natl Acad Sci USA* 1998; 95: 831–838
- Goodlett CB, Fletcher PT, Gilmore JH, Gerig G: Group analysis of DTI fiber tract statistics with application to neurodevelopment. *Neuroimage* 2009; 45(suppl):S133–S142
- Rueckert D, Sonoda LI, Hayes C, Hill DL, Leach MO, Hawkes DJ: Nonrigid registration using free-form deformations: application to breast MR images. *IEEE Trans Med Imaging* 1999; 18:712–721
- Joshi S, Davis B, Jomier M, Gerig G: Unbiased diffeomorphic atlas construction for computational anatomy. *Neuroimage* 2004; 23(suppl 1):S151–S160
- Salvador R, Peña A, Menon DK, Carpenter TA, Pickard JD, Bullmore ET: Formal characterization and extension of the linearized diffusion tensor model. *Hum Brain Mapp* 2005; 24:144–155
- Alexander DC, Pierpaoli C, Basser PJ, Gee JC: Spatial transformations of diffusion tensor magnetic resonance images. *IEEE Trans Med Imaging* 2001; 20:1131–1139
- Fletcher PT, Joshi S: Riemannian geometry for statistical analysis of diffusion tensor data. *Signal Processing* 2007; 87:250–262
- Mori S, Wakana S, Nagae-Poetscher LM, van Zijl PCM: MRI Atlas of Human White Matter. Amsterdam, Elsevier, 2005
- Song SK, Sun SW, Ramsbottom MJ, Chang C, Russell J, Cross AH: Demyelination revealed through MRI as increased radial (but unchanged axial) diffusion of water. *Neuroimage* 2002; 17: 1429–1436
- Wake H, Lee PR, Fields RD: Control of local protein synthesis and initial events in myelination by action potentials. *Science* 2011; 333:1647–1651
- Mädler B, Drabycz SA, Kolind SH, Whittall KP, MacKay AL: Is diffusion anisotropy an accurate monitor of myelination? Correlation of multicomponent T2 relaxation and diffusion tensor

- anisotropy in human brain. *Magn Reson Imaging* 2008; 26: 874–888
33. Braddick O, Atkinson J, Hood B, Harkness W, Jackson G, Vargha-Khadem F: Possible blindsight in infants lacking one cerebral hemisphere. *Nature* 1992; 360:461–463
  34. Deoni SCL, Dean DC 3rd, O’Muircheartaigh J, Dirks H, Jerskey BA: Investigating white matter development in infancy and early childhood using myelin water fraction and relaxation time mapping. *Neuroimage* 2012; 63:1038–1053
  35. LaMantia AS, Rakic P: Axon overproduction and elimination in the corpus callosum of the developing rhesus monkey. *J Neurosci* 1990; 10:2156–2175
  36. Wheeler-Kingshott CA, Cercignani M: About “axial” and “radial” diffusivities. *Magn Reson Med* 2009; 61:1255–1260
  37. Frick JE, Colombo J, Saxon TF: Individual and developmental differences in disengagement of fixation in early infancy. *Child Dev* 1999; 70:537–548
  38. Colombo J, Shaddy DJ, Richman WA, Maikranz JM, Blaga OM: The developmental course of habituation in infancy and pre-school outcome. *Infancy* 2004; 5:1–38
  39. Mosconi MW, Kay M, D’Cruz AM, Guter S, Kapur K, Macmillan C, Stanford LD, Sweeney JA: Neurobehavioral abnormalities in first-degree relatives of individuals with autism. *Arch Gen Psychiatry* 2010; 67:830–840
  40. Dawson G: Early behavioral intervention, brain plasticity, and the prevention of autism spectrum disorder. *Dev Psychopathol* 2008; 20:775–803
  41. Elsabbagh M, Mercure E, Hudry K, Chandler S, Pasco G, Charman T, Pickles A, Baron-Cohen S, Bolton P, Johnson MH; BASIS Team: Infant neural sensitivity to dynamic eye gaze is associated with later emerging autism. *Curr Biol* 2012; 22: 338–342
  42. Wolff JJ, Gu H, Gerig G, Elison JT, Styner M, Gouttard S, Botteron KN, Dager SR, Dawson G, Estes AM, Evans AC, Hazlett HC, Kostopoulos P, McKinstry RC, Paterson SJ, Schultz RT, Zwaigenbaum L, Piven J; IBIS Network: Differences in white matter fiber tract development present from 6 to 24 months in infants with autism. *Am J Psychiatry* 2012; 169:589–600
  43. Wass S, Porayska-Pomsta K, Johnson MH: Training attentional control in infancy. *Curr Biol* 2011; 21:1543–1547